In-silico genome-scale metabolic modeling and in-vitro static time-kill studies of exogenous metabolites alone and with polymyxin B against Klebsiella pneumoniae

Wan Yean Chung[1], Nusaibah Abdul Rahim[2], Mohd Hafidz Mahamad Maifiah[3], Naveen Kumar Hawala Shivashekaregowda[1], Yan Zhu[4*], Eng Hwa Wong[1*]

[1]Taylor's University, Malaysia, [2]University of Malaya, Malaysia, [3]International Islamic University Malaysia, Malaysia, [4]Monash University, Australia

Submitted to Journal:
Frontiers in Pharmacology

Specialty Section:
Pharmacology of Infectious Diseases

Article type:
Original Research Article

Manuscript ID:
880352

Received on:
21 Feb 2022

Revised on:
16 May 2022

Journal website link:
www.frontiersin.org

Conflict of interest statement

The authors declare that the research was conducted in the absence of any commercial or financial relationships that could be construed as a potential conflict of interest

Author contribution statement

All authors listed have made a substantial, direct and intellectual contribution to the work and approved it for publication.

Keywords

Klebsiella pneumoniae, polymyxin, metabolite, Genome-scale metabolic modeling, time-kill, Metabolic modulation

Abstract

Word count: 253

Multidrug-resistant (MDR) Klebsiella pneumoniae is a top-prioritized Gram-negative pathogen with a high incidence in hospital acquired infections. Polymyxins have resurged as a last-line therapy to combat Gram-negative 'superbugs' including MDR K. pneumoniae. However, emergence of polymyxin resistance has increasingly been reported over the past decades when used as monotherapy and thus combination therapy with non-antibiotics (e.g., metabolites) becomes a promising approach owing to lower risk of resistance development. Genome-scale metabolic models were constructed to delineate the altered metabolism of New Delhi metallo-ß-lactamase or extended spectrum ß-lactamase producing K. pneumoniae strains upon addition of exogenous metabolites in media. The metabolites caused significantly metabolic perturbations were then selected to examine their adjuvant effects using in-vitro static time-kill studies. Metabolic network simulation shows that feeding of 3-phosphoglycerate and ribose 5-phosphate would lead to enhanced central carbon metabolism, ATP demand and energy consumption, which is converged with metabolic disruptions by polymyxin treatment. Further static time-kill studies demonstrated enhance antimicrobial killing of 10 mM 3-phosphoglycerate (1.26 and 1.82 log10 CFU/mL) and 10 mM ribose 5-phosphate (0.53 and 0.91 log10 CFU/mL) combination with 2 mg/L polymyxin B against K. pneumoniae strains. Overall, exogenous metabolite feeding could possibly improve polymyxin B activity via metabolic modulation and hence offers an attractive approach to enhance polymyxin B efficacy. With the application of GSMM in bridging the metabolic analysis and time-kill assay, biological insights of metabolite feeding can be inferred from comparative analyses of both results. Taken together, a systematic framework has been developed to facilitate the clinical translation of antibiotic-resistant infections management.

Contribution to the field

Emergence of multidrug resistant Klebsiella pneumoniae are reported at an alarming rate. Polymyxins have resurged as the last-line drugs. The use combination therapy with non-antibiotic, metabolite, is a promising approach to curb the resistance. Metabolomic studies revealed that antibiotic therapy caused regulation of metabolites abundance and affected the bacterial metabolic state. Following this line of thought, genome-scale metabolic models (GSMM) were constructed to elucidate the bacterial metabolism of K. pneumoniae strains upon addition of exogenous metabolite. Metabolic pathways that significantly perturbed according to GSMM were then selected for in-vitro time-kill studies. GSMM shows that feeding of 3-phosphoglycerate, glycerol 3-phosphate, D-ribose 5-phosphate and uridine 5□-diphospho-N-acetylglucosamine would lead to enhanced central carbon metabolism, ATP demand and energy consumption, which is converged with metabolic disruptions by polymyxin treatment. Further static time-kill studies demonstrated enhance antimicrobial killing of 10 mM 3-phosphoglycerate (1.26 and 1.82 log10 CFU/mL), 10 mM ribose 5-phosphate (0.53 and 0.91 log10 CFU/mL) and 1 mM uridine 5□-diphospho-N-acetylglucosamine (0.70 log10 CFU/mL) combination with 2 mg/L polymyxin B against K. pneumoniae strains. Overall, exogenous metabolite feeding could possibly improve polymyxin B activity via metabolic modulation. With the application of GSMM in bridging the metabolic analysis and time-kill assay, biological insights of metabolite feeding can be inferred from comparative analyses of both results. Taken together, a systematic framework has been developed to facilitate the clinical translation of antibiotic-resistant infections management.

Funding statement

This work was supported by the Fundamental Research Grant Scheme, Ministry of Higher Education, Malaysia [FRGS/1/2019/SKK11/TAYLOR/03/1].

Ethics statements

Studies involving animal subjects
Generated Statement: No animal studies are presented in this manuscript.

Studies involving human subjects
Generated Statement: No human studies are presented in this manuscript.

Inclusion of identifiable human data
Generated Statement: No potentially identifiable human images or data is presented in this study.

Data availability statement

Generated Statement: The original contributions presented in the study are included in the article/supplementary material, further inquiries can be directed to the corresponding author/s.

In-silico genome-scale metabolic modeling and *in-vitro* static time-kill studies of exogenous metabolites alone and with polymyxin B against *Klebsiella pneumoniae*

Wan Yean Chung[1], Nusaibah Abdul Rahim[2], Mohd Hafidz Mahamad Maifiah[3], Naveen Kumar Hawala Shivashekaregowda[4], Yan Zhu[5*], Eng Hwa Wong[6*]

[1]School of Pharmacy, Taylor's University, 47500 Subang Jaya, Selangor, Malaysia

[2]Faculty of Pharmacy, University of Malaya, 50603 Kuala Lumpur, Malaysia

[3]International Institute for Halal Research and Training (INHART), International Islamic University Malaysia (IIUM), 53100 Jalan Gombak, Selangor, Malaysia

[4]Center for Drug Discovery and Molecular Pharmacology (CDDMP), Faculty of Health and Medical Sciences, Taylor's University, 47500 Subang Jaya, Selangor, Malaysia

[5]Biomedicine Discovery Institute, Infection Program and Department of Microbiology, Monash University, Melbourne, Victoria 3800, Australia

[6]School of Medicine, Taylor's University, 47500 Subang Jaya, Selangor, Malaysia

*** Correspondence:**
Dr Eng Hwa Wong
enghwa.wong@taylors.edu.my

Dr Yan Zhu
yan.zhu@monash.edu

Number of words: 3654 words

Number of tables: 2

Number of figures: 3

Keywords: *Klebsiella pneumoniae*, polymyxin, metabolite, genome-scale metabolic modeling, time-kill, metabolic modulation

Abstract

Multidrug-resistant (MDR) *Klebsiella pneumoniae* is a top-prioritized Gram-negative pathogen with a high incidence in hospital acquired infections. Polymyxins have resurged as a last-line therapy to combat Gram-negative 'superbugs' including MDR *K. pneumoniae*. However, emergence of polymyxin resistance has increasingly been reported over the past decades when used as monotherapy and thus combination therapy with non-antibiotics (e.g., metabolites) becomes a promising approach owing to lower risk of resistance development. Genome-scale metabolic models were constructed to delineate the altered metabolism of New Delhi metallo-β-lactamase or extended spectrum β-lactamase producing *K. pneumoniae* strains upon addition of exogenous metabolites in media. The metabolites caused significantly metabolic perturbations were then selected to examine their adjuvant effects using *in-vitro* static time-kill studies. Metabolic network simulation shows that feeding of 3-phosphoglycerate and ribose 5-phosphate would lead to enhanced central carbon metabolism, ATP demand and energy consumption, which is converged with metabolic disruptions by polymyxin treatment. Further static time-kill studies demonstrated enhance antimicrobial killing of 10 mM 3-phosphoglycerate (1.26 and 1.82 $\log_{10}$ CFU/mL) and 10 mM ribose 5-phosphate (0.53 and 0.91 $\log_{10}$ CFU/mL) combination with 2 mg/L polymyxin B against *K. pneumoniae* strains. Overall, exogenous metabolite feeding could possibly improve polymyxin B activity via metabolic modulation and hence offers an attractive approach to enhance polymyxin B efficacy. With the application of GSMM in bridging the metabolic analysis and time-kill assay, biological insights of metabolite feeding can be inferred from comparative analyses of both results. Taken together, a systematic framework has been developed to facilitate the clinical translation of antibiotic-resistant infections management.

1 Introduction

Emergence of multidrug-resistant (MDR) bacterial pathogens, including carbapenem-resistant *Klebsiella pneumoniae*, has garnered regular warnings of World Health Organization (World Health Organization, 2020) and U.S. Centers for Disease Control and Prevention (U.S. Centers for Disease Control and Prevention, 2021). Polymyxins (i.e., polymyxin B and colistin) are a group of lipopeptide antibiotics that are used as a last resort to treat severe infections caused by Gram-negative 'superbugs'. Resistance can emerge during polymyxin monotherapy, which is mainly mediated by lipid A modifications in *K. pneumoniae* (Baron *et al.*, 2016). Recently, the increasing prevalence of mobile resistance gene *mcr* in *Enterobacterales* places critical challenges to polymyxins use (Liu *et al.*, 2016; Yang *et al.*, 2018; Hadjadj *et al.*, 2019), underlining the urgent need for novel antimicrobial therapeutic strategy. In clinic, colistin and polymyxin B are either used alone or in combination with other antimicrobials, to treat life-threatening infection due to carbapenem-resistance *K. pneumoniae* (Nang *et al.*, 2021; Yang *et al.*, 2021). The emergence of polymyxin resistance in *K. pneumoniae* clinical isolates through diverse genetic adaptation has renewed research focus on the importance of combination therapy. Furthermore, the polymyxin dosage is limited by their nephrotoxicity and neurotoxicity (Aggarwal and Dewan, 2018). Combination therapies of polymyxin antibiotics are often employed to inhibit the resistance emergence and minimize the potential toxicity (Bergen *et al.*, 2019). Among the combination treatments, using non-antibiotic adjuvant such as exogenous metabolites together with polymyxin B is a promising approach as the use of metabolite at low concentrations is generally non-toxic to the host (Cheng *et al.*, 2014; Zeng *et al.*, 2017; Jiang *et al.*, 2020; Rosenberg, Fang and Allison, 2020; Wang *et al.*, 2020).

Recent studies have demonstrated that cellular metabolism of bacterial pathogens is critical for antimicrobial efficacy (Liu *et al.*, 2019). Modulation of cellular metabolism via exogenous

metabolite feeding could significantly elevate antibiotic susceptibility of drug-resistant bacteria (Zeng *et al.*, 2017; Su *et al.*, 2018; Yang *et al.*, 2019). However, the complicated interplay of multiple metabolic pathways underlying the synergy of metabolite-antimicrobial combination remains unclear, thus hampering the discovery of effective metabolite adjuvant to improve antimicrobial efficacy, including the last-line polymyxins. Genome-scale metabolic model (GSMM) serves as a systematic tool to simulate metabolic flux changes in response to antimicrobial treatment and metabolite feeding (Wadhwa *et al.*, 2018; Rizvi *et al.*, 2019; Zhou *et al.*, 2021), and thus it can assist to delineate the mechanisms of enhanced bacterial killing by exogenous metabolite feeding.

The primary aim of this study is to identify promising polymyxin B-metabolite combinations against MDR *K. pneumoniae* using GSMM coupled with time-kill studies. Four GSMMs were constructed to elucidate the metabolic adaptation of *K. pneumoniae* strains upon addition of metabolite. We reveal that rewiring of metabolic flux distribution occurred owing to the feeding of additional metabolites. We also show that increased antimicrobial activity was demonstrated by the combination of 3-phosphoglycerate (3PG) and ribose 5-phosphate (R5P) with polymyxin B against New Delhi metallo-β-lactamase (NDM) and extended spectrum β-lactamase (ESBL) producing isolates.

2 Materials and Methods

2.1 Bacterial isolates

Four *K. pneumoniae* American Type Culture Collection (ATCC) isolates were analysed: ATCC 10031, 700603 (ST489, Pasteur scheme, same for following strains), 700721 (ST38, also known as *K. pneumoniae* MGH78578) and BAA-2146 (ST11). The strains were selected to represent a mixture of strains susceptible and resistant to polymyxin B (**Table 1**) and MDR strains. Strain ATCC 700603 was originally isolated from urine sample of a hospitalized patient in 1994 (Elliott *et al.*, 2016) and produces multiple ESBLs, specifically beta-lactamase SHV-18. Strain ATCC BAA-2146 is a NDM producing reference strain. All strains were purchased from ATCC and were stored in tryptone soy broth with 20% glycerol at -80℃.

2.2 Genome-scale metabolic modeling

The draft models were initially constructed by CarveMe (Machado *et al.*, 2018) using genome annotation and coded in System Biology Markup Language Level 3 Version 1 (Hucka *et al.*, 2010). Manual curation and metabolic simulations were performed using COBRApy (Ebrahim *et al.*, 2013). Transport and exchange reactions were added to allow nutrient uptake and metabolite transport across membranes according to BiGG database (Norsigian *et al.*, 2020). The manually added metabolites were complemented with specific properties including compartment localization, charge, formula, name and database identifier according to the BiGG database.

For simulation of bacterial growth in minimal media (M9), the maximum uptake rates of nutrient ingredients were set to 10 $mmol \cdot gDW^{-1} \cdot h^{-1}$ (Zhu *et al.*, 2018). Whereas for Mueller-Hinton (MH) medium, the maximum uptake rates of nutrient ingredient were empirically constrained to 1 $mmol \cdot gDW^{-1} \cdot h^{-1}$ (Zhu *et al.*, 2019). Non-growth associated maintenance ATP consumption was set to 10 $mmol \cdot gDW^{-1} \cdot h^{-1}$ according to previous study (Zhu *et al.*, 2018).

Seven exogenous metabolites tested in this study are phenylpyruvate (PHPYR), orotate (OROT), 3-phosphohydroxypyruvate (3PHP), glycerol 3-phosphate (GLYC3P), 3PG, R5P and uridine 5′-diphospho-*N*-acetylglucosamine (UACGAM). MH medium was used for metabolic modelling. For each metabolite, additional transport reactions were incorporated to the draft model, and the

maximum uptake rate was constrained to 10 mmol·gDW^{-1}·h^{-1}. Metabolic solution space was sampled with 10,000 random points using OptgpSampler (Megchelenbrink, Huynen and Marchiori, 2014). Flux distributions of metabolite feeding were then compared with those of non-feeding conditions.

2.3 Antibiotic and exogenous metabolites

Polymyxin B was purchased from Merck (Darmstadt, Hesse) and was prepared by dissolving with Milli-Q water to obtain a final concentration of 512 mg/L. The exogenous metabolites (10 mM PHPYR, 1 mM OROT, 5mM 3PHP, 10 mM 3PG, 10 mM R5P and 1mM UACGAM) were individually examined, alone and in combination with 2 mg/L polymyxin B against the four *K. pneumoniae* strains by static time-kill studies. The concentrations of exogenous metabolites were normalized to deliver 60 mM carbon except OROT, 3PHP and 3PG due to their poor aqueous solubility. All metabolites were purchased from Sigma-Aldrich (Saint Louis, Missouri).

2.4 Static time-kill studies

Static time-kill studies were conducted over 24 h to study antimicrobial activity and emergence of resistance after treatment with polymyxin B (Lin *et al.*, 2019; Wistrand-Yuen *et al.*, 2020). *K. pneumoniae* isolates were investigated at an initial inoculum of 10^6 CFU/mL [standard inoculum, as per Clinical and Laboratory Standards Institute (CLSI) guidelines]. Log-phase cultures of *K. pneumoniae* isolates were prepared prior to the experiments.

Before spiking in antimicrobial agents, a sample of t=0 h was collected. Clinically relevant free unbound concentration of polymyxin B, 2 mg/L was used. After spiking in antimicrobial agents, further samples (~700 µL) at t=1, 4 and 24 h were collected aseptically, diluted appropriately in 0.9% saline solution, and plated manually. Upon incubation at 35°C for 24 h, viable cell counting was conducted. The final cell viability was expressed in $\log_{10}$ CFU/mL.

Polymyxin B exerted rapid bactericidal activity within 1 h, but significant bacterial regrowth was observed following 24 h exposure to polymyxin B monotherapy (Lin *et al.*, 2019). Hence, the pharmacodynamic effect of the combination treatment was assessed over 24 h to investigate bacterial regrowth. Findings from polymyxin B pharmacokinetic studies suggest a currently recommended mean polymyxin B maximum serum concentration at steady-state ranges from ~2–14 mcg/mL (Avedissian *et al.*, 2019). The polymyxin B concentrations selected were based on the clinical dosing regimens (Tsuji *et al.*, 2019).

2.5 Pharmacodynamic analysis

Pharmacodynamic analysis was carried out to determine microbiological response to antimicrobial treatment (Lin Y-W, 2019). The log change method (log change = [$\log_{10}(CFU_t) - \log_{10}(CFU_0)$]) was used, comparing change in bacterial count from 0 h to time point of interest. For static time-kill studies, antibacterial activity involves a reduction of ≥1 $\log_{10}$ CFU/mL from the initial inoculum. Bactericidal activity was defined as ≥ 3 $\log_{10}$ CFU/mL reduction from the starting inoculum. Additivity and synergy were defined as 1.0 to <2 $\log_{10}$ CFU/mL and ≥2 log10 CFU/mL reduction with the combination relative to its most active single agent, respectively (Sharma *et al.*, 2017). Antagonism was defined as ≥1 $\log_{10}$ CFU/mL increase between the combination and the most active single agent (Shields *et al.*, 2018; Barber *et al.*, 2021).

3 Results

3.1 Construction of genome-scale metabolic models for selected *K. pneumoniae* strains

With the aim of identifying promising metabolite adjuvants to increase antimicrobial activity of polymyxin B against *K. pneumoniae*, we have studied polymyxin-resistant strain ATCC 10031, polymyxin-susceptible strain ATCC 700721, and polymyxin-susceptible but MDR *K. pneumoniae* strains (ATCC 700603 and BAA-2146) (**Table 1)**. In addition, GSMMs were constructed to simulate flux changes upon metabolite addition. Initial draft models were developed for the four *K. pneumoniae* isolates based on genome annotation. During manual curation against literature and databases, a total of 10-12 metabolites and 20-23 reactions were added for each model **(Table S1)**, enabling metabolite uptake and secretion. The resulting models were designated iKpne_ATCC10031_21 (ATCC 10031), iKpne_ATCC700603_21 (ATCC 700603), iKpne_ATCCBAA2146_21 (ATCC BAA-2146) and iKpne_ATCC700721_21 (ATCC 700721) according to naming convention, and each of them contains 2,531–2,713 reactions, 1,695–1,778 metabolites and 1,292–1,612 genes (**Table 2**).

3.2 Genome-scale metabolic modeling

The four models predicted the maximum specific growth rate (μ_{max}) of 0.92 and 1.05 h^{-1} in M9 and MH media, respectively. The predicted μ_{max} in MH media ia similar with the calculated μ_{max} using time-kill data which varied between 1.02-1.16 h^{-1} for the *K. pneumoniae* isolates.

The metabolites were selected based on previous transcriptomic and metabolomic findings (Rahim *et al.*, 2016; Maifiah *et al.*, 2017; Han *et al.*, 2018; Hussein *et al.*, 2018), which indicated that the intracellular levels of metabolites R5P, UACGAM and GLYC3P were significantly perturbed by polymyxin. Furthermore, metabolites PHPYR, OROT, 3PG and 3PHP have also been identified as significant metabolites perturbed by the combination (Rahim *et al.*, 2016). Although many significant metabolites were identified from the studies, the selected metabolites were those that demonstrated perturbations to both gene expression and metabolism of the same pathway [e.g., *gnd* and R5P in pentose phosphate pathway (PPP); *pgk* and 3PG in gluconeogenesis] by the combination (Rahim *et al.*, 2016; Abdul Rahim *et al.*, 2020). For instance, transcriptomics and metabolomics results revealed that expression of gene *gnd* and abundance level of R5P were downregulated and decreased in response to the polymyxin combination treatment, respectively. Thus, these observations were believed to further strengthen the basis of selection.

GSMM simulations results show that addition of PHPYR, OROT and 3PHP resulted in limited impact on non-central metabolic pathways; whereas feeding of 3PG, GLYC3P, R5P and UACGAM induced significant metabolic perturbations to multiple pathways including central metabolism (**Figure 1**). GLYC3P was excluded for further analyses due to its similar impact as 3PG. The perturbed reaction specific flux values under control and metabolite feeding treatment are denoted in the format $\mathbf{flux_{control}/flux_{metabolite}}$ in brackets in **section 3.2.1** and **3.2.2**.

3.2.1 Metabolic impact on non-central metabolism

The model simulations predict that the uptake of exogenous PHPYR was at a relatively low rate compared to other metabolites and exerted minimal effect on phenylalanine metabolism upon feeding. Generally, GSMM results show addition of OROT would increase pyrimidine biosynthesis. Higher flux distribution of orotate phosphoribosyltransferase (ORPT) (iKpne_ATCC10031_21: 0.41/0.54; iKpne_ATCC700603_21: 0.20/0.43; iKpne_ATCC700721_21: 0.22/0.48; iKpne_ATCCBAA2146_21: 0.19/0.42), orotidine 5'-phosphate decarboxylase (OMPDC) (iKpne_ATCC10031_21: 0.41/0.54; iKpne_ATCC700603_21: 0.20/0.43; iKpne_ATCC700721_21: 0.22/0.48; iKpne_ATCCBAA2146_21:0.19/0.42) and uridine 5′-monophosphate kinase (UMPK) (iKpne_ATCC10031_21: 1.67/1.76; iKpne_ATCC700603_21: 2.64/2.87; iKpne_ATCC700721_21: 2.57/2.58; iKpne_ATCCBAA2146_21: 2.59/2.65) indicated elevated pyrimidine biosynthesis activity. Uridine diphosphate (UDP) was further converted to uridine-5'-triphosphate (UTP) via higher flux through nucleoside-diphosphate kinase (NDPK2) (iKpne_ATCC10031_21: 5.99/6.17; iKpne_ATCC700603_21: 4.92/5.20; iKpne_ATCC700721_21: 4.65/4.55; iKpne_ATCCBAA2146_21: 5.18/5.14). Moreover, the addition of exogenous 3PHP was predicted to digest into serine and glycine metabolism to increase fluxes of phosphoserine transaminase (PSERT) (iKpne_ATCC10031_21: 2.29/11.43; iKpne_ATCC700603_21: 0.89/10.67; iKpne_ATCC700721_21: 1.47/10.62; iKpne_ATCCBAA2146_21: 1.29/10.57), phosphoserine phosphatase (PSP_L) (iKpne_ATCC10031_21: 2.29/11.43; iKpne_ATCC700603_21: 0.89/10.67; iKpne_ATCC700721_21: 1.47/10.62; iKpne_ATCCBAA2146_21: 1.29/10.57), and then glycine hydroxymethyltransferase (GHMT2r) (iKpne_ATCC10031_21: -1.11/6.00; iKpne_ATCC700603_21: -2.15/4.33; iKpne_ATCC700721_21: -1.27/4.98; iKpne_ATCCBAA2146_21: -0.90/6.04) to form glycine.

3.2.2 Metabolic impact on central metabolism

GSMM results show that feeding of 3PG resulted in increased glycolytic/gluconeogenetic fluxes in all four strains **(Figure 1).** Results show that 3PG influx bifurcates to form D-glycerate 2-phosphate (2PG) of glycolysis and 3-Phospho-D-glyceroyl phosphate (13DPG) of gluconeogenesis; the latter in turn enhanced PPP flux to generate R5P. Results show enhanced production of PRPP, the starting metabolite of nucleotide biosynthesis pathway (**Figure 1**) and increased fluxes of reactions ORPT, OMPDC, UMPK and NDPK2 towards UTP biosynthesis. Furthermore, addition of 3PG was predicted to increase serine biosynthesis via enhanced fluxes of PSERT (iKpne_ATCC10031_21: 2.29/5.39; iKpne_ATCC700603_21: 0.89/3.70; iKpne_ATCC700721_21: 1.47/3.85; iKpne_ATCCBAA2146_21: 1.29/4.43) and PSP_L (iKpne_ATCC10031_21: 2.29/5.39; iKpne_ATCC700603_21: 0.89/3.70; iKpne_ATCC700721_21: 1.47/3.85; iKpne_ATCCBAA2146_21: 1.29/4.43). Increased of TCA cycle flux was observed upon feeding of 3PG. Additionally, the overall fluxes within oxidative phosphorylation were increased (**Figure 2**) which potentially resulted in higher oxygen consumption and higher ATP turnover rate.

Furthermore, the GSMM predicted the exogenous GLYC3P formed dihydroxyacetone phosphate (DHAP) through enhanced dehydrogenation (iKpne_ATCC10031_21: -4.15/4.26; iKpne_ATCC700603_21: -4.92/1.80; iKpne_ATCC700721_21: -3.92/3.95; iKpne_ATCCBAA2146_21: -4.15/3.06), which in turn flew down to glycolysis, serine metabolism and eventually to the TCA cycle (**Figure 1**). The metabolic flux changes caused by GLYC3P feeding are similar to 3PG feeding. In addition, feeding of R5P was predicted to significantly affect central carbon metabolism flux. The addition of R5P would preferably to form D-ribulose 5-phosphate (RU5P) than PRPP via isomerisation (iKpne_ATCC10031_21: -0.44/5.80; iKpne_ATCC700603_21: -2.42/1.48; iKpne_ATCC700721_21: -2.59/0.54; iKpne_ATCCBAA2146_21: -2.56/1.19). Increased

flux of generating fructose 6-phosphate (F6P) from RU5P would enter glycolysis metabolism, then the end product of glycolysis, acetyl CoA, was fueled to the TCA cycle for cellular respiration. Furthermore, the GSMM results also reveal feeding of UACGAM increased fluxes of central and nucleotide metabolism. The exogenous UACGAM flow into PPP through nucleotide salvage pathway (**Figure 1**) via increased flux of pyrimidine-nucleoside phosphorylase (iKpne_ATCC700603_21: -1.42/6.54; iKpne_ATCC700721_21: -1.32/6.40; iKpne_ATCCBAA2146: -1.00/6.91) except for iKpne_ATCC10031_21. Model iKpne_ATCC10031 predicted exogenous UACGAM digested into PPP via increased flux of uridine hydrolase (URIH) (iKpne_ATCC10031_21: 0.44/9.85).

3.3 Validation of metabolite effects using *in vitro* time-kill

Polymyxin B (2 mg/L) monotherapy produced rapid and extensive killing within 1 h against all isolates except ATCC 10031 with ≥ 3 $\log_{10}$ CFU/mL killing (**Figure 3A-B**). Nevertheless, significant bacterial regrowth was observed at 24 h for all isolates treated with polymyxin B monotherapy.

For the six metabolites tested, three metabolites-polymyxin B combinations demonstrated enhanced antimicrobial activity against MDR *K. pneumoniae* isolates even when NDM was present.

The combination of polymyxin B (2 mg/L) with 10 mM 3PG resulted in strong bacterial killing at 1 h with 4.3 – 6.2 $\log_{10}$ CFU/mL reduction for isolate ATCC 700603 and BAA-2146 compared to initial inoculum (**Figure 3A**). At 4 h, the combination treatment increased the extent of antibacterial activity approximately to 2 $\log_{10}$ CFU/mL (1.82 $\log_{10}$ CFU/mL) reduction for isolate ATCC 700603 relatives to its most active polymyxin B monotherapy (**Figure 3A**). Similar increased antibacterial effect was also observed for the combination treatment against MDR isolate BAA-2146 with 1.26 $\log_{10}$ CFU/mL reduction at 4 h (**Figure 3A**). However, bacterial regrowth was observed for both isolates at 24 h.

Metabolite feeding with 10 mM R5P combined with polymyxin B showed a bacterial count reduction of approximately 1 $\log_{10}$ CFU/mL (0.91 $\log_{10}$ CFU/mL) for isolate ATCC 700721 (**Figure 3B**). Interestingly, isolate ATCC 10031 is resistant to polymyxin B monotherapy and addition of R5P to polymyxin B resulted in a modest improvement in antibacterial activity with 0.53 $\log_{10}$ CFU/mL reduction compared with polymyxin B monotherapy at 4 h (**Figure 3B**).

The antibacterial effect of UACGAM feeding was also tested against MDR isolates. For ESBL isolate ATCC 700603, addition of 1 mM UACGAM to polymyxin B treatment showed an increase of bacterial killing of 1 $\log_{10}$ CFU/mL reduction. The magnitude of antibacterial activity was further enhanced to 0.70 log10 CFU/ml reduction at 4 h in contrast to polymyxin B monotherapy (**Figure S1**).

4 Discussion

The rapid spread of opportunistic *K. pneumoniae* that are resistant to last-resort polymyxins highlights the urgent requirement for novel antimicrobial adjuvant therapy to minimize the emergence of resistance. Polymyxin B combination with non-antibiotic, such as metabolites offers an attractive approach to increase antibacterial activity without exceeding the clinically achieved concentration of polymyxin B. To this end, it is crucial to understand the reciprocal relationship of bacterial metabolic responses to exogenous metabolites and antimicrobial activity to optimize the combination therapy. GSMM is a powerful tool in studying bacterial metabolism and it has been applied to elucidate mechanism of antibiotic killing and development of resistance, thus integration

with *in-vitro* experiments enables a systematic framework for identifying novel exogenous metabolite-antibiotic combination.

Simulation with the four GSMMs showed that additions of exogenous metabolites such as 3PG, 3PHP, GLYC3P, R5P and UACGAM display effect on increasing bacterial growth except for metabolite PHPYR and OROT. This could be explained by the flow of metabolic flux corresponding to the metabolite addition where metabolite PHPYR was not digested in the metabolism; OROT addition only exerted minor effects on purine and pyrimidine metabolism. The highest growth induced by UACGAM feeding among the metabolites demonstrated the highest metabolic flux changes in model predictions. The uridine part of UACGAM can be digested to form nucleotides whereas the amino sugar component (i.e., *N*-acetyl glucosamine) was utilised for cell envelope biosynthesis.

Growth rate is the primary variable that determines the phenotype of susceptibility to antibiotics of the bacterial populations (Martínez and Rojo, 2011). Slow growth rate was associated with low antibiotic activity (Yang, Bening and Collins, 2017; Zampieri *et al.*, 2017; Lee *et al.*, 2018) thus we hypothesize the stagnant bacterial growth upon feeding of PHPYR and OROT would not exert antibacterial activity when treated together with polymyxin B against *K. pneumoniae* isolates. The time-kill studies supported this hypothesis where both combination therapies (i.e., polymyxin B with PHPYR; polymyxin B with OROT) did not show effect on antibacterial activity. In addition, minor metabolic flux changes in glucose metabolism and oxidative phosphorylation displayed by feeding of these two metabolites suggest that no metabolic regulating and modulation occur.

Prax *et al*. (2016) had shown glucose potentiated a membrane-active antimicrobial peptide, daptomycin killing may be dependent on glucose metabolism (Prax *et al.*, 2016). The attenuation of carbon catabolism associated with cellular respiration is the primary cause in metabolite-driven ciprofloxacin activity (Gutierrez *et al.*, 2017). Recent metabolomics results showed polymyxins treatment induced dramatic changes in central carbon metabolism in polymyxin-susceptible Gram-negative pathogens (Maifiah *et al.*, 2017; Zhu *et al.*, 2019). Our fluxomic data revealed metabolite feeding of 3PG, R5P, UACGAM and GLYC3P notably increased glycolysis, PPP and TCA cycle fluxes. It is conceivable that exogenous metabolite feeding would further intensify metabolic burden attributed to the polymyxin B activity and cause increased cellular respiration. On top of that, polymyxin treatment also induced disruption to nucleotides biosynthesis (Zhu *et al.*, 2018). *In-silico* addition of the aforementioned four metabolites also upregulated purine and pyrimidine metabolism. Our time-kill result showed enhanced antimicrobial killing by the combination of 3PG, R5P and UACGAM treated along with polymyxin B against *K. pneumoniae* (**Figure 3A-B and S1**). These results indicate that the surge of ATP required to restore the disrupted nucleotide pool because of both antibiotic and metabolite treatments (Yang *et al.*, 2019). The enhanced ATP demand stimulating the nucleotide biosynthesis metabolism, elevated central carbon metabolism. The increased metabolic activity by metabolite feeding is likely to produce toxic metabolic by-products that reduce bacterial fitness (Stokes *et al.*, 2019), hence increasing the killing effect of polymyxin B.

Another possible mechanism of the metabolite feeding is increased production of reactive oxygen species (ROS) to enhance antibiotic activity (Brynildsen *et al.*, 2013; Van Acker and Coenye, 2017). Increasing ROS production would increase bacterial sensitivity to oxidative attack (Brynildsen *et al.*, 2013). ~~This resulted in impairment of detoxification and repair system of bacteria and might led to enhanced killing by the oxidants and antibiotic (Brynildsen *et al.*, 2013).~~ The mechanism of polymyxin action involves free radical-induced death (Trimble *et al.*, 2016). Abdul Rahim *et al.* (2016) postulated an increase in nucleotide synthesis including R5P and OROT was an initial

bacterial stress response to polymyxin combination treatment (Rahim *et al.*, 2016). Such metabolic perturbation might exacerbate by driven TCA activity upon metabolite feeding. Our results showed metabolite feeding upregulated TCA cycle and produced NADH which is utilized for facilitating electron transport chain. This would induce the formation of ROS and cause oxidative damage contributing to lethality. ~~Cells produce ROS such as superoxide anion, hydrogen peroxide and hydroxy radical by extracting electrons from molecular oxygen through enzyme activity. These endogenous ROS species can cause damage to DNA, lipids and proteins, thereby compelling pathogen to protect themselves against lethality with stress responses (Juan *et al.*, 2021). When both polymyxin B and exogenous metabolite enter across bacteria cell wall, the antibacterial activity might trigger the oxidants level to increase. Eventually it would stimulate oxidative damage of biological molecules with deleterious effects on the cell when the concentration of oxidants reaches a significant level. Hence, it is plausible to conclude exogenous metabolite that induced TCA cycle activity such as 3PG, GLYC3P, R5P and UACGAM will contribute to ROS-mediated cell death.~~ Altogether, the increased fluxes of NADH16pp, FADRx and CYTBDpp (**Figure 2**) inducing an oxidative stress and concurrently increased metabolic activity by metabolite feeding may sensitize *K. pneumoniae* to polymyxin B killing.

For polymyxin B-resistant isolate ATCC 10031, evident in time-kill studies, the addition of metabolite R5P to polymyxin B resulted in slight improvement (log change = 0.52 $\log_{10}$ CFU/mL) in antibacterial activity at 4 h compared with polymyxin B monotherapy (**Figure 3B**). This suggests that metabolite feeding may be a possible approach to restore antibiotic susceptibility of antibiotic-resistant isolates. Antibiotic-resistant strains generally demonstrated to have weaker bacterial fitness and reduced metabolism due to evolution of mutation under selection pressure of antibiotic (Lázár *et al.*, 2014). The addition of exogenous metabolites to restore the metabolic deprivation offers a hopeful approach to increase sensitivity to antibiotics of antibiotic-resistant bacteria (Cheng *et al.*, 2019; Li *et al.*, 2020). This enables better antimicrobial activity to be achieved with combinations containing clinically relevant polymyxin B concentrations given that polymyxin B induced nephrotoxicity is a dose-limiting adverse effect (Avedissian *et al.*, 2019).

Despite the positive antimicrobial effect of the combination treatment, an antagonistic effect was observed for combination of 3PG and R5P with polymyxin B against ATCC 10031 and ATCC 700603, respectively (**Figure 3A-B**). Although the underlying mechanisms of these antagonism pairs remain unclear, it could be considered as a potential target for the development of new antimicrobial therapy of these *K. pneumoniae* isolates. Alteration of related metabolic processes could thereby lead to revert of the antagonistic effect thus improving the susceptibility of antibiotics. It would be interesting to investigate the metabolic perturbations in the gene expression and metabolism in the *K. pneumoniae* isolates driven by the combination.

In summary, this is the first study incorporating GSMM findings to unveil mechanistic insights into metabolic flux changes following metabolite addition, correlated antibiotic activity through *in-vitro* studies. This will shed light on antimicrobial development on non-antibiotic combination to polymyxin B to rescue the last-line resort. Further studies into transcriptomics and metabolomics analysis to delineate the complex metabolic responses to metabolite feeding are warranted for better model validation and accuracy. Apart from that, *in-vivo* studies are crucial to evaluate the efficacy, concentration and safety of metabolite adjuvants used in potentiating antibiotic activity against MDR *K. pneumoniae* infections.

Conflict of Interest

The authors declare that the research was conducted in the absence of any commercial or financial relationships that could be construed as a potential conflict of interest.

Funding

This work was supported by the Fundamental Research Grant Scheme, Ministry of Higher Education, Malaysia [FRGS/1/2019/SKK11/TAYLOR/03/1].

References

Abdul Rahim, N. *et al.* (2020) 'Transcriptomic responses of a New Delhi metallo-β-lactamase-producing *Klebsiella pneumoniae* isolate to the combination of polymyxin B and chloramphenicol', *International Journal of Antimicrobial Agents*, 56(2), p. 106061. doi: 10.1016/J.IJANTIMICAG.2020.106061.

Van Acker, H. and Coenye, T. (2017) 'The Role of Reactive Oxygen Species in Antibiotic-Mediated Killing of Bacteria', *Trends in Microbiology*, 25(6), pp. 456–466. doi: 10.1016/J.TIM.2016.12.008.

Aggarwal, R. and Dewan, A. (2018) 'Comparison of nephrotoxicity of Colistin with Polymyxin B administered in currently recommended doses: A prospective study', *Annals of Clinical Microbiology and Antimicrobials*, 17(1), pp. 1–8. doi: 10.1186/S12941-018-0262-0/TABLES/6.

Avedissian, S. N. *et al.* (2019) 'A review of the clinical pharmacokinetics of polymyxin B', *Antibiotics*, 8(1), pp. 1–11. doi: 10.3390/antibiotics8010031.

Barber, K. E. *et al.* (2021) 'Biofilm Time-Kill Curves to Assess the Bactericidal Activity of Daptomycin Combinations against Biofilm-Producing Vancomycin-Resistant *Enterococcus faecium* and *faecalis*', *Antibiotics 2021, Vol. 10, Page 897*, 10(8), p. 897. doi: 10.3390/ANTIBIOTICS10080897.

Baron, S. *et al.* (2016) 'Molecular mechanisms of polymyxin resistance: knowns and unknowns', *International Journal of Antimicrobial Agents*, 48(6), pp. 583–591. doi: 10.1016/J.IJANTIMICAG.2016.06.023.

Bergen, P. J. *et al.* (2019) Rational Combinations of Polymyxins with Other Antibiotics, *Advances in Experimental Medicine and Biology*. doi: 10.1007/978-3-030-16373-0_16.

Brynildsen, M. P. *et al.* (2013) 'Potentiating antibacterial activity by predictably enhancing endogenous microbial ROS production', *Nature biotechnology*, 31(2), p. 160. doi: 10.1038/NBT.2458.

Cheng, Z. *et al.* (2019) 'Glycine, serine and threonine metabolism confounds efficacy of complement-mediated killing', *Nature Communications 2019 10:1*, 10(1), pp. 1–17. doi: 10.1038/s41467-019-11129-5.

Cheng, Z. xue *et al.* (2014) 'N-acetylglucosamine enhances survival ability of tilapias infected by *Streptococcus iniae*', *Fish and Shellfish Immunology*, 40(2), pp. 524–530. doi: 10.1016/j.fsi.2014.08.008.

Ebrahim, A. *et al.* (2013) 'COBRApy: COnstraints-Based Reconstruction and Analysis for Python', *BMC Systems Biology 2013 7:1*, 7(1), pp. 1–6. doi: 10.1186/1752-0509-7-74.

Elliott, A. G. *et al.* (2016) 'Complete Genome Sequence of *Klebsiella quasipneumoniae* subsp. *similipneumoniae* Strain ATCC 700603', *Genome Announcements*, 4(3). doi: 10.1128/GENOMEA.00438-16.

Gutierrez, A. *et al.* (2017) 'Understanding and Sensitizing Density-Dependent Persistence to Quinolone Antibiotics', *Molecular Cell*, 68(6), pp. 1147-1154.e3. doi: 10.1016/j.molcel.2017.11.012.

Hadjadj, L. *et al.* (2019) 'Co-occurrence of Variants of mcr-3 and mcr-8 Genes in a *Klebsiella pneumoniae* Isolate From Laos', *Frontiers in Microbiology*, 10, p. 2720. doi: 10.3389/FMICB.2019.02720/BIBTEX.

Han, M. L. *et al.* (2018) 'Metabolic analyses revealed time-dependent synergistic killing by colistin and aztreonam combination against multidrug-resistant *Acinetobacter baumannii*', *Frontiers in Microbiology*, 9(NOV), p. 2776. doi: 10.3389/FMICB.2018.02776/BIBTEX.

Hucka, M. *et al.* (2010) 'The Systems Biology Markup Language (SBML): Language Specification for Level 3 Version 1 Core', *Nature Precedings 2010*, pp. 1–1. doi: 10.1038/npre.2010.4959.1.

Hussein, M. *et al.* (2018) 'Mechanistic Insights From Global Metabolomics Studies into Synergistic Bactericidal Effect of a Polymyxin B Combination With Tamoxifen Against Cystic Fibrosis MDR *Pseudomonas aeruginosa*', *Computational and Structural Biotechnology Journal*, 16, pp. 587–599. doi: 10.1016/J.CSBJ.2018.11.001.

Jiang, M. *et al.* (2020) 'Exogenous maltose enhances Zebrafish immunity to levofloxacin-resistant *Vibrio alginolyticus*', *Microbial Biotechnology*, 13(4), pp. 1213–1227. doi: 10.1111/1751-7915.13582.

Lázár, V. *et al.* (2014) 'Genome-wide analysis captures the determinants of the antibiotic cross-resistance interaction network', *Nature Communications 2014 5:1*, 5(1), pp. 1–12. doi: 10.1038/ncomms5352.

Lee, A. J. *et al.* (2018) 'Robust, linear correlations between growth rates and β-lactam-mediated lysis rates', *Proceedings of the National Academy of Sciences of the United States of America*, 115(16), pp. 4069–4074. doi: 10.1073/PNAS.1719504115/-/DCSUPPLEMENTAL.

Li, L. *et al.* (2020) 'Metabolic mechanism of colistin resistance and its reverting in *Vibrio alginolyticus*', *Environmental Microbiology*, 22(10), pp. 4295–4313. doi: 10.1111/1462-2920.15021.

Lin Y-W, A. R. N. (2019) 'Novel Polymyxin Combination with the Antiretroviral Zidovudine Exerts Synergistic Killing against NDM-Producing', *Antimicrobial Agents and Chemotherapy*, 63(4), pp. 1–11.

Lin, Y. W. *et al.* (2019) 'Novel polymyxin combination with the antiretroviral zidovudine exerts synergistic killing against NDM-producing multidrug-resistant *Klebsiella pneumoniae*', *Antimicrobial Agents and Chemotherapy*, 63(4). doi: 10.1128/AAC.02176-18/SUPPL_FILE/AAC.02176-18-S0001.PDF.

Liu, Y. *et al.* (2019) 'Bacterial metabolism-inspired molecules to modulate antibiotic efficacy', *Article in Journal of Antimicrobial Chemotherapy*. doi: 10.1093/jac/dkz230.

Liu, Y. Y. *et al.* (2016) 'Emergence of plasmid-mediated colistin resistance mechanism MCR-1 in animals and human beings in China: a microbiological and molecular biological study', *The Lancet Infectious Diseases*, 16(2), pp. 161–168. doi: 10.1016/S1473-3099(15)00424-7.

Machado, D. *et al.* (2018) 'Fast automated reconstruction of genome-scale metabolic models for microbial species and communities', *Nucleic Acids Research*, 46(15), pp. 7542–7553. doi: 10.1093/NAR/GKY537.

Maifiah, M. H. M. *et al.* (2017) 'Untargeted metabolomics analysis reveals key pathways responsible for the synergistic killing of colistin and doripenem combination against *Acinetobacter baumannii*', *Scientific Reports*, 7(February), pp. 1–12. doi: 10.1038/srep45527.

Martínez, J. L. and Rojo, F. (2011) 'Metabolic regulation of antibiotic resistance', *FEMS Microbiology Reviews*, 35(5), pp. 768–789. doi: 10.1111/J.1574-6976.2011.00282.X.

Megchelenbrink, W., Huynen, M. and Marchiori, E. (2014) 'optGpSampler: An Improved Tool for Uniformly Sampling the Solution-Space of Genome-Scale Metabolic Networks', *PLoS ONE*, 9(2). doi: 10.1371/JOURNAL.PONE.0086587.

Nang, S. C. *et al.* (2021) 'Rescuing the Last-Line Polymyxins: Achievements and Challenges', *Pharmacological Reviews*, 73(2), pp. 679–728. doi: 10.1124/pharmrev.120.000020.

Norsigian, C. J. *et al.* (2020) 'BiGG Models 2020: multi-strain genome-scale models and expansion across the phylogenetic tree', *Nucleic Acids Research*, 48(D1), pp. D402–D406. doi: 10.1093/NAR/GKZ1054.

Prax, M. *et al.* (2016) 'Glucose augments killing efficiency of daptomycin challenged *Staphylococcus aureus* persisters', *Plos One*, 11(3), p. e0150907. doi: 10.1371/JOURNAL.PONE.0150907.

Rahim, N. A. *et al.* (2016) 'Integrative Multi-Omics Network Analysis of the Synergistic Killing of Polymyxin B and Chloramphenicol in Combination Against an NDM-producing *Klebsiella pneumoniae* Isolate', in *2016 European Congress of Clinical Microbiology and Infectious Diseases (ECCMID)*, p. EV0651.

Rizvi, A. *et al.* (2019) 'Rewiring of metabolic network in *Mycobacterium tuberculosis* during adaptation to different stresses', *Frontiers in Microbiology*, 10(OCT), p. 2417. doi: 10.3389/FMICB.2019.02417/BIBTEX.

Rosenberg, C. R., Fang, X. and Allison, K. R. (2020) 'Potentiating aminoglycoside antibiotics to reduce their toxic side effects', *PLOS ONE*, 15(9), p. e0237948. doi: 10.1371/JOURNAL.PONE.0237948.

Sharma, R. *et al.* (2017) 'Polymyxin B in combination with meropenem against carbapenemase-producing *Klebsiella pneumoniae*: pharmacodynamics and morphological changes', *International Journal of Antimicrobial Agents*, 49(2), pp. 224–232. doi: 10.1016/J.IJANTIMICAG.2016.10.025.

Shields, R. K. *et al.* (2018) 'Colistin does not potentiate ceftazidime-avibactam killing of carbapenem-resistant *enterobacteriaceae in vitro* or suppress emergence of ceftazidime-avibactam resistance', *Antimicrobial Agents and Chemotherapy*, 62(8), pp. 1018–1036. doi: 10.1128/AAC.01018-18/ASSET/31C2B56B-AA14-4E65-BD27-B7E2094C9C41/ASSETS/GRAPHIC/ZAC0081873750002.JPEG.

Stokes, J. M. *et al.* (2019) 'Bacterial metabolism and antibiotic efficacy', *Cell Metabolism*, 30(2), pp. 251–259. doi: 10.1016/j.cmet.2019.06.009.

Su, Y. bin *et al.* (2018) 'Pyruvate cycle increases aminoglycoside efficacy and provides respiratory energy in bacteria', *Proceedings of the National Academy of Sciences of the United States of America*, 115(7), pp. E1578–E1587. doi: 10.1073/pnas.1714645115.

Trimble, M. J. *et al.* (2016) 'Polymyxin: alternative mechanisms of action and resistance', *Cold Spring Harbor Perspectives in Medicine*, 6(10), p. a025288. doi: 10.1101/CSHPERSPECT.A025288.

Tsuji, B. T. *et al.* (2019) 'International consensus guidelines for the optimal use of the polymyxins: endorsed by the American College of Clinical Pharmacy (ACCP), European Society of Clinical Microbiology and Infectious Diseases (ESCMID), Infectious Diseases Society of America (IDS', *Pharmacotherapy: The Journal of Human Pharmacology and Drug Therapy*, 39(1), pp. 10–39. doi: 10.1002/PHAR.2209.

U.S. Centers for Disease Control and Prevention (2021) *About Antibiotic Resistance | Antibiotic/Antimicrobial Resistance | CDC*. Available at: https://www.cdc.gov/drugresistance/about.html (Accessed: 25 November 2021).

Wadhwa, M. *et al.* (2018) 'Role of phosphate limitation and pyruvate decarboxylase in rewiring of the metabolic network for increasing flux towards isoprenoid pathway in a TATA binding protein mutant of *Saccharomyces cerevisiae*', *Microbial Cell Factories*, 17(1), pp. 1–14. doi: 10.1186/S12934-018-1000-1/FIGURES/6.

Wang, M. *et al.* (2020) 'N-Acetyl-D-Glucosamine acts as adjuvant that re-sensitizes starvation-induced antibiotic-tolerant population of *E. Coli* to β-lactam', *iScience*, 23(11), p. 101740. doi: 10.1016/J.ISCI.2020.101740.

Wistrand-Yuen, P. *et al.* (2020) 'Evaluation of polymyxin B in combination with 13 other antibiotics against carbapenemase-producing *Klebsiella pneumoniae* in time-lapse microscopy and time-kill experiments', *Clinical Microbiology and Infection*, 26(9), pp. 1214–1221. doi: 10.1016/J.CMI.2020.03.007.

World Health Organization (2020) *Antibiotic resistance*. Available at: https://www.who.int/news-room/fact-sheets/detail/antibiotic-resistance (Accessed: 25 November 2021).

Yang, J. H. *et al.* (2019) 'A white-box machine learning approach for revealing antibiotic mechanisms of action', *Cell*, 177(6), pp. 1649-1661.e9. doi: 10.1016/j.cell.2019.04.016.

Yang, J. H., Bening, S. C. and Collins, J. J. (2017) 'Antibiotic efficacy — context matters', *Current Opinion in Microbiology*, 39, pp. 73–80. doi: 10.1016/J.MIB.2017.09.002.

Yang, X. *et al.* (2021) 'Carbapenem resistance-encoding and virulence-encoding conjugative

plasmids in *Klebsiella pneumoniae*', *Trends in Microbiology*, 29(1), pp. 65–83. doi: 10.1016/J.TIM.2020.04.012.

Yang, Y. Q. *et al.* (2018) 'Novel plasmid-mediated colistin resistance gene mcr-7.1 in *Klebsiella pneumoniae*', *Journal of Antimicrobial Chemotherapy*, 73(7), pp. 1791–1795. doi: 10.1093/JAC/DKY111.

Zampieri, M. *et al.* (2017) 'Nontargeted metabolomics reveals the multilevel response to antibiotic perturbations', *Cell Reports*, 19(6), pp. 1214–1228. doi: 10.1016/J.CELREP.2017.04.002.

Zeng, Z. hai *et al.* (2017) 'Glucose enhances tilapia against *Edwardsiella tarda* infection through metabolome reprogramming', *Fish and Shellfish Immunology*, 61, pp. 34–43. doi: 10.1016/j.fsi.2016.12.010.

Zhou, J. *et al.* (2021) 'Advances in the development of constraint-based genome-scale metabolic network models', *Chinese Journal of Biotechnology*, 37(5), pp. 1526–1540. doi: 10.13345/J.CJB.200498.

Zhu, Y. *et al.* (2018) 'Genome-scale metabolic modeling of responses to polymyxins in *Pseudomonas aeruginosa*', *GigaScience*, 7(4), pp. 1–18. doi: 10.1093/gigascience/giy021.

Zhu, Y. *et al.* (2019) ' Metabolic responses to polymyxin treatment in *Acinetobacter baumannii* ATCC 19606: Integrating transcriptomics and metabolomics with Genome-scale metabolic modeling ', *mSystems*, 4(1), pp. 1–15. doi: 10.1128/msystems.00157-18.

Table 1. MICs of *K. pneumoniae* isolates

***K. pneumoniae* isolate**	**Polymyxin B MIC (mg/L)**
ATCC 10031	4
ATCC 700603	2
ATCC 700721	2
ATCC BAA-2146	2

Table 2. Total number of genes, metabolites and reactions in the constructed GSMMs.

GSMM	Gene	Metabolite	Reaction
iKpne_ATCC10031_21	1292	1703	2531
iKpne_ATCC700603_21	1612	1778	2708
iKpne_ATCC700721_21	1587	1778	2713
iKpne_ATCCBAA2146_21	1572	1695	2611

Figure 1. Metabolite feeding of 3PG, GLYC3P, R5P and UACGAM induced metabolic alterations. The subgraphs indicate the distribution of sampled metabolic fluxes (mmol·gDW^{-1}·h^{-1}) in iKpne_ATCC700603_21 (blue, control; orange, 3PG; grey, GLYC3P; red, R5P; green, UACGAM). The metabolite abbreviations are as follows: g6p, D-glucose 6-phosphate; f6p, D-fructose 6-phosphte; fdp, D-fructose 1,6-biphosphate; dhap, dihydroxyacetone phosphate; g3p, glyceraldehyde 3-phosphate; 13dpg, 3-phospho-D-glyceroyl phosphate; 3pg, 3-phosphoglycerate; 2pg, D-glycerate 2-phosphate; pep, phosphoenolpyruvate; pyr, pyruvate; ru5p, D-ribulose 5-phosphate; xu5p, D-xylulose 5-phosphate; r5p, D-ribose 5-phosphate; s7p, sedoheptulose 7-phosphate; e4p, D-erythrose 4-phosphate; prpp, 5- phospho-alpha-D-ribose 1-diphosphate; 3php, 3-phosphohydroxypyruvate; ser_L, L-serine; gly, glycine; mal_L, L-malate; oaa, oxaloacetate; cit, citrate; acon_C, cis-aconitate; icit, isocitrate; akg, 2-oxoglutarate; succoa, succinyl-CoA; succ, succinate; fum, fumarate. The reaction abbreviations are as follows: FBP, fructose-bisphosphatase; PGK, phosphoglycerate kinase; PGM, phosphoglycerate mutase; TKT2, transketolase 2; RPI, ribose-5-phosphate isomerase; PRPPS, phosphoribosylpyrophosphate synthetase; PGCD, phosphoglycerate dehydrogenase; PSP_L, phosphoserine phosphatase; ACONTa, aconitase (half-reaction A); AKGDH, 2-oxoglutarate dehydrogenase

Figure 2. Oxidative phosphorylation fluxes changes upon metabolite addition. The reaction abbreviations are as follows: NADH16pp, NADH dehydrogenase (ubiquinone-8 and 3 protons) (periplasm); FADRx, FAD reductase; CYTBDpp, cytochrome oxidase bd (ubiquinol-8: 2 protons) (periplasm).

Figure 3. Time-kill curves of metabolite treatment with polymyxin B (PMB), alone and in combination. **(A)** 10 mM 3PG **(B)** 10 mM R5P

Figure S1: Time-kill curves of UACGAM treatment with polymyxin B (PMB), alone and in combination.

Figure 1.TIFF

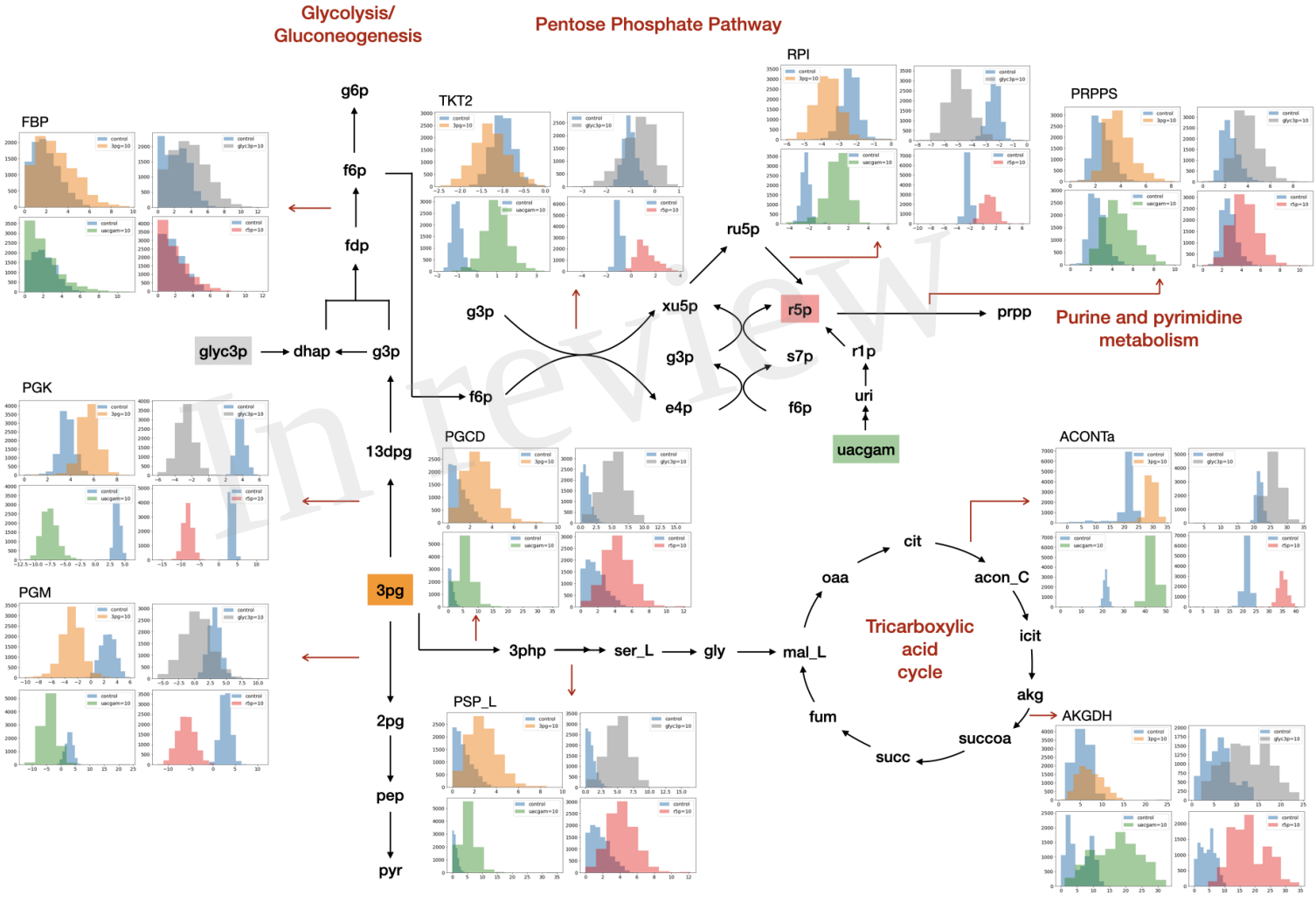

Figure 2.TIFF

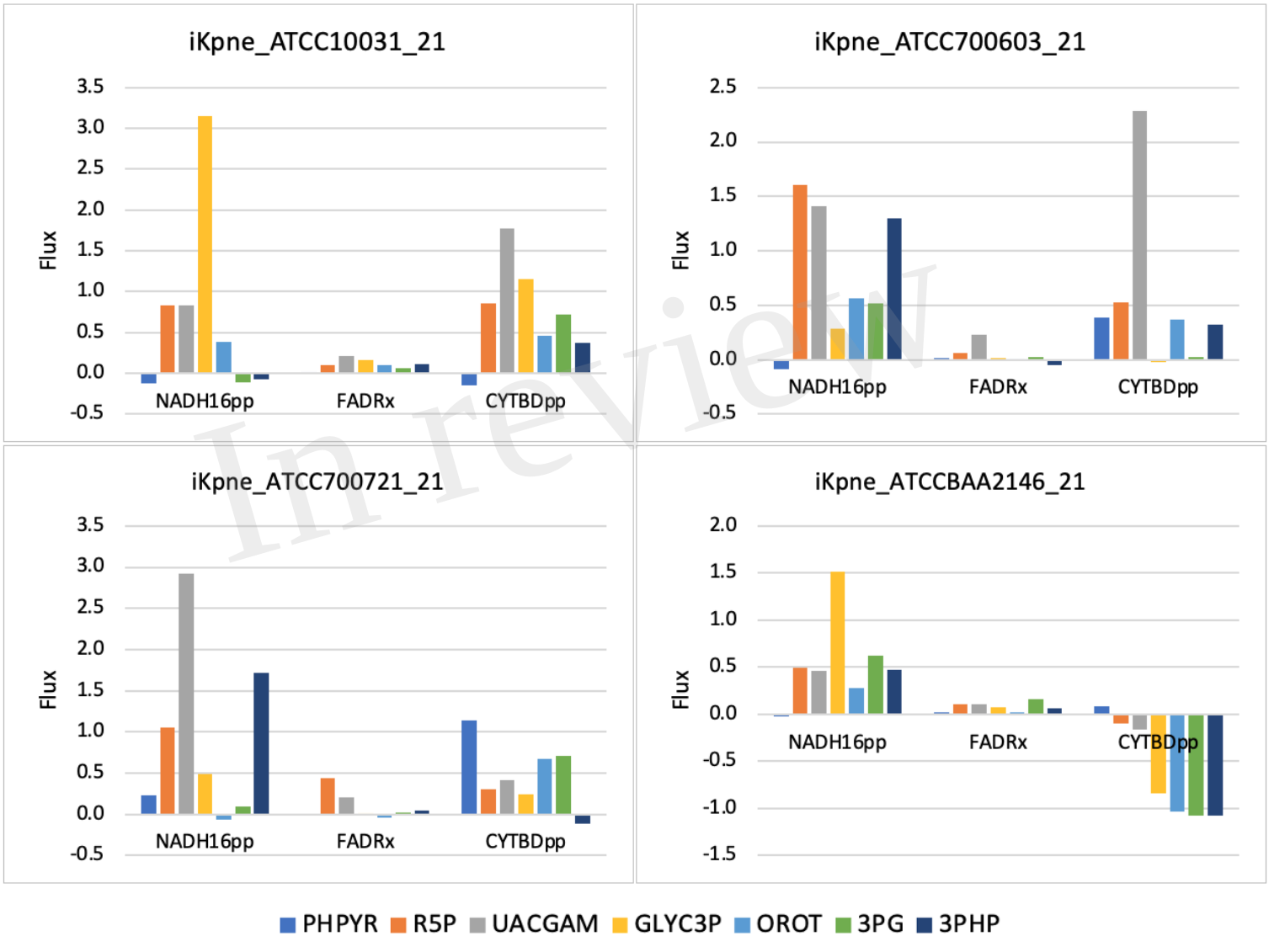

Figure 3.TIFF